

FULL PAPER

Open Access



# Geophysical imaging of subsurface structures in volcanic area by seismic attenuation profiling

Tetsuro Tsuru<sup>1\*</sup> , Tetsuo No<sup>2</sup> and Gou Fujie<sup>2</sup>

## Abstract

Geophysical imaging by using attenuation property of multichannel seismic reflection data was tested to map spatial variation of physical properties of rocks in a volcanic area. The study area is located around Miyakejima volcanic island, where an intensive earthquake swarm was observed associated with 2000 Miyakejima eruption. Seismic reflection survey was conducted five months after the swarm initiation in order to clarify crustal structure around the hypocenters of the swarm activity. However, the resulting seismic reflection profiles were unable to provide significant information of deep structures around the hypocenters. The authors newly applied a seismic attribute method that focused seismic attenuation instead of reflectivity to the volcanic area, and designed this paper to assess the applicability of this method to subsurface structural studies in poorly reflective volcanic areas. Resulting seismic attenuation profiles successfully figured out attenuation structures around the Miyakejima volcanic island. Interestingly, a remarkable high-attenuation zone was detected between Miyakejima and Kozushima islands, being well correlated with the hypocenter distribution of the earthquake swarm in 2000. The high-attenuation zone is interpreted as a fractured area that was developed by magma activity responsible for the earthquake swarms that have been repeatedly occurring there. The present study can be one example showing the applicability of seismic attenuation profiling in a volcanic area.

**Keywords:** Seismic attenuation, Poorly reflective, Volcanic, Earthquake swarm, Miyakejima

## Background

As a high-resolution geophysical imaging technique to figure out subsurface structures, seismic reflection survey has been widely used in the areas of oil and gas explorations and crustal studies. Seismic reflection profiles are the most general product, enabling us to visually recognize formation boundaries as continuous reflections. Moreover, the seismic reflection amplitude provides the physical properties of rocks such as acoustic impedance as well as type of pore fluid in subsurface.

However, it is difficult to deduce the subsurface structures from reflection profiles collected in less reflective areas: volcanic area and highly faulted area where continuous reflections are inherently difficult to be observed.

Therefore, several techniques, but not many, have been tested: seismic attribute analysis (e.g., Tokuyama et al. 1988), seismic scattering analysis (Mikada et al. 1997). These methods focused on some attributes other than reflection amplitude and successfully detected subsurface information. From the same point of view, we applied a seismic attribute using attenuation property, “seismic attenuation profiling (SAP)” (Tsuru and No 2011; Tsuru et al. 2014), in a volcanic area between Miyakejima, Kozushima and Niijima island volcanos in Japan.

The objective of the present study is to image a highly fractured zone that was possibly caused by earthquake swarm activity associated with Miyakejima eruption in 2000. Although seismic attenuation is well investigated in studies using VSP data (e.g., Hauge 1981; Worthington and Hudson 2000), well log data (e.g., Matsushima 2006) and core samples (e.g., Tompkins and Christensen 2001; Tsuji and Iturrino 2008), it is rarely applied to surface seismic reflection data except previous studies on

\*Correspondence: [ttsuru0@kaiyodai.ac.jp](mailto:ttsuru0@kaiyodai.ac.jp)

<sup>1</sup> Academic Assembly, Tokyo University of Marine Science and Technology (TUMSAT), 5-7, Konan 4-chome, Minato-ku, Tokyo 108-8477, Japan  
Full list of author information is available at the end of the article

a direct hydrocarbon indication (Dasgupta and Clark 1998), a fault seal ability evaluation (Tsuru et al. 2014) and  $Q$  tomography/migration for oil and gas industry (e.g., Zhou et al. 2011).

## Methods

The SAP method is a technique to image seismic attenuation structure from seismic reflection data (Tsuru and No 2011; Tsuru et al. 2014). The method has an advantage in application to geophysical imaging or rock property estimation of less reflective areas such as volcanic area and highly faulted area, because it does not require continuous reflections. On the other hand, the present SAP method using spectral ratio has a disadvantage in resolution because it requires an averaging process to mitigate the influences from abnormal values caused by local noises: About 100 samples and 15 traces are used in vertical direction and horizontal direction, respectively, in the present study.

In the present study, the assumption that  $Q$  is constant over the seismic frequency band was adopted as many previous authors did (e.g., Knopoff 1964), although some other studies found indications for frequency-dependent  $Q$  (e.g., Mavko and Nur 1979). From the viewpoint of investigating attenuation effect from seismic field data, one should remove other effects in advance: geometrical spreading, scattering, noises and so on. However, it is actually impossible to remove them completely. Moreover,  $Q$  values computed in the present study is the so-called effective  $Q$  ( $Q_{\text{eff}}$ ), which is the sum of the inelastic absorption  $Q_i$  and the apparent attenuation  $Q_a$  (Spencer et al. 1982) given by

$$\frac{1}{Q_{\text{eff}}} = \frac{1}{Q_i} + \frac{1}{Q_a}. \quad (1)$$

Namely, the SAP method is not capable of separating  $Q_i$  and  $Q_a$ . Although a direct correlation between  $Q_{\text{eff}}$  and a special rock type is difficult,  $Q_{\text{eff}}$  gives information about changes in lithology and fluid property, being a valuable aid in geological interpretation (Tonn 1991; Dasgupta and Clark 1998; Zhou et al. 2011).

First we calculated average  $Q$  value by the spectral ratio method, which is known as one of the most general methods to estimate  $Q$  (e.g., Hauge 1981; Tonn 1991; Dasgupta and Clark 1998). Temporal decay in amplitude of a propagating seismic wave of frequency  $f$  from travel-time  $t_1$  to traveltime  $t_2$  can be written by a function of  $Q$ :

$$A_{t_2}(f) = A_{t_1}(f) \exp \left[ -\frac{\pi f \delta t}{Q} \right] \quad (2)$$

where  $\delta t = t_2 - t_1$ .  $A_{t_1}$  and  $A_{t_2}$  are amplitude spectrum of wavelet at  $t_1$  and that at  $t_2$ , respectively. By adding geometrical spreading effect  $G$  and reflection coefficient

$R$  (Dasgupta and Clark 1998), Eq. (2) can be written as follows:

$$A_{t_2}(f) = GRA_{t_1}(f) \exp \left[ -\frac{\pi f \delta t}{Q} \right], \quad (3)$$

then

$$\frac{A_{t_2}(f)}{A_{t_1}(f)} = GR \exp \left[ -\frac{\pi f \delta t}{Q} \right]. \quad (4)$$

Taking the logarithm of both sides:

$$\ln \left[ \frac{A_{t_2}(f)}{A_{t_1}(f)} \right] = -\frac{\pi f \delta t}{Q} + \ln(GR) = pf + \ln(GR), \quad (5)$$

where

$$p = -\frac{\pi \delta t}{Q}. \quad (6)$$

Since the logarithm of spectral ratio of a wavelet at  $t_2$  and that at  $t_1$  is a linear function of frequency  $f$  as expressed in Eq. (5), an effective  $Q$  can be computed from its gradient “ $p$ ” by Eq. (6).

In general, the spectral ratio method uses two each of amplitude spectrums that are calculated in two each of time windows consecutively set on seismic records. However, this method is very sensitive to noise (Tonn 1991). Previous authors therefore coped with this issue by some ways. For example, Dasgupta and Clark (1998) used only limited area of seismic reflection data around the area of interest in  $Q$  calculation. Tsuru et al. (2014) used a stacked seismic record and adopted amplitude spectrums of seafloor reflections as the denominator of the left side of Eq. (5). In the present study, amplitude spectrums of the uppermost part of the area of interest were used as the denominator (Appendix Fig. 12). On the other hand, the numerator spectrums were calculated in time windows set from top to bottom of seismic reflection profile.

As another step to cope with noise, we selected a frequency band for the gradient “ $p$ ” computation by the following criterion.

- (1) Effective frequency band of input data

Prior to SAP calculation, a band-pass filter of 5–50 Hz was applied in the data processing. Therefore, the frequency band width for “ $p$ ” computation must be set within the pass band of 5–50 Hz.

- (2) Ghost notch

Ghost notch is one of the obstacles that should be taken care in computing “ $p$ ” because of lower signal level at notch frequency. In the present study, the input seismic data were collected with a streamer cable of 20 m towing

depth and an air-gun array of 10 m towing depth. Consequently, the ghost notches were caused at the frequencies of 0, 37.5, 75 Hz and so on. Therefore, 5–37.5 Hz and/or 37.5–50 Hz are candidates for the frequency band width for the “*p*” computation.

### (3) Dominant frequency range of reflections

Dominant frequency range of the input seismic reflection data is 20–30 Hz. Therefore, the frequency band of 5–37.5 Hz is more appropriate than 37.5–50 Hz.

### (4) Frequency dependency of attenuation

Seismic wave attenuates more largely in proportion to the increase of frequency. In other words, attenuation can be easily detected with higher frequency. Therefore, we finally selected 21–37.5 Hz, which is higher half of the 5–37.5 Hz, as the “*p*” computation band. Thus, we assumed that *Q* was constant within such a narrow frequency band.

Within the frequency band of 21–37.5 Hz, average *Q* values were computed along a stacked seismic trace at every CDP. Spectrum of the denominator of the left side of Eq. (5) was computed within a time window of the traveltimes between 2.5 and 3.0 s at every CDP, which approximately corresponds to the uppermost part of the volcanic rocks in the study area. Spectrum of the numerator was computed within each time window, which was set on the seismic trace one by one from top to bottom. Then a seismic attenuation profile (SAP) was created.

Furthermore, interval *Q* can be calculated from average *Q* by the following equation (e.g., Tonn 1991):

$$\frac{t_{k-1,k}}{Q_{\text{int},k}} = \frac{t_{I,k}}{Q_{\text{ave},I,k}} - \frac{t_{I,k-1}}{Q_{\text{ave},I,k-1}}, \quad (7)$$

where  $Q_{\text{int},k}$  is interval *Q* of *k*th time window and  $t_{k-1,k}$  is two-way traveltimes between *k*th and *k* – 1th time windows.  $Q_{\text{ave},I,k}$  is average *Q* between the uppermost part of the area of interest and *k*th time window, and  $t_{I,k}$  is two-way traveltimes between them. Subsequently, a seismic attenuation profile of interval *Q* was produced.

## Study area and data specifications

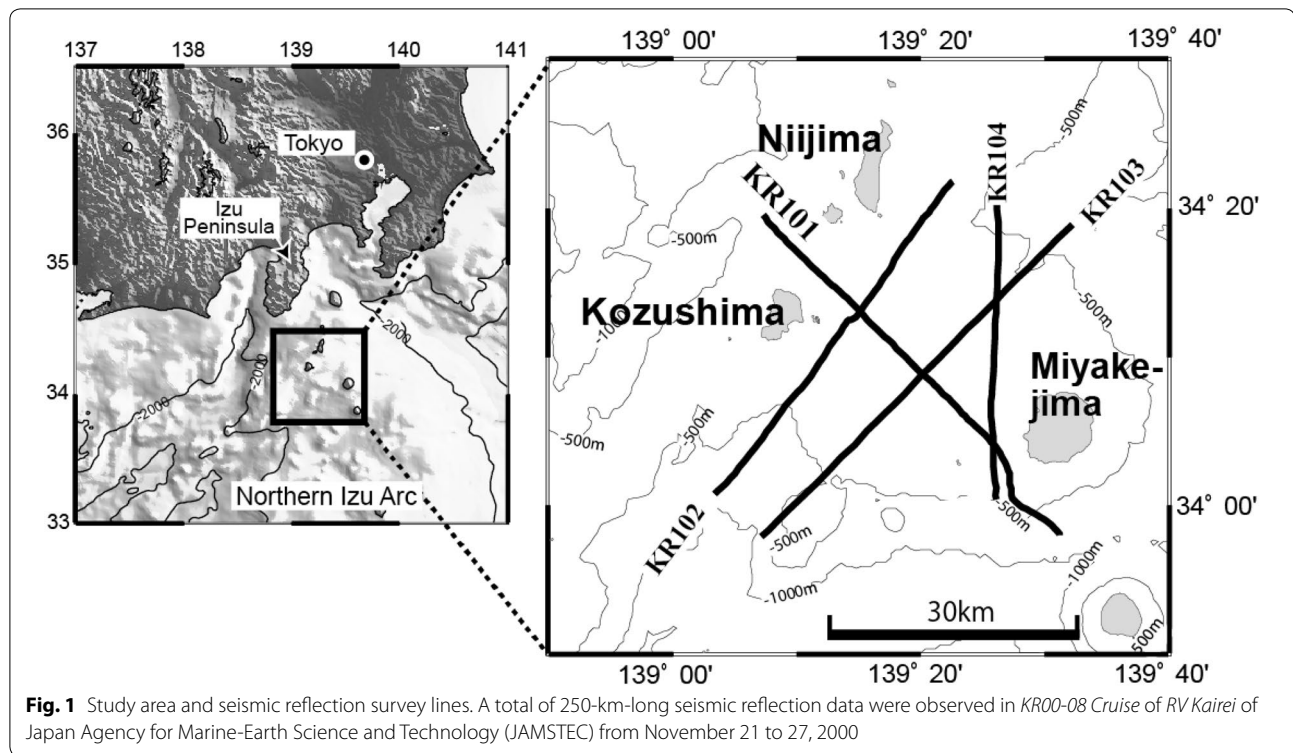
The study area is located around Miyakejima and Kozushima volcanic islands about 170 km south of Tokyo, Japan (Fig. 1). The volcanic islands belong to the Izu islands, where volcanic activities accompanied by earthquake swarms have been repeatedly occurring (Mogi 1963;

Tsukui and Suzuki 1998; Hamada 2001). Regarding hypocenter depths of the earthquake swarms before 2000, Hamada et al. (1985) reported that the hypocenters of the 1962 swarm between Miyakejima and Kozushima were distributed around 20 km in depth. However, they also noted a possibility of 10 km. Due to limited observation networks, firm hypocenter depths were not clarified between the two islands until 2000.

On June 26, 2000, small volcanic earthquakes began to be recorded at observation stations west of the summit of the Miyakejima volcano, and subsequently an earthquake swarm initiated (Sakai et al. 2001). The swarm migrated northwestward toward the direction of Kozushima and Niiijima and then developed the most intense earthquake swarm ever observed in and around Japanese archipelago (Japan Meteorological Agency 2000; Uhira et al. 2005). The main eruption of the Miyakejima volcano occurred at the summit on July 8, 2000 (e.g., Sakai et al. 2001). A number of earthquakes occurred during a period of these two months (Nishizawa et al. 2002). The hypocenter depths of the 2000 swarm activity between Miyakejima and Kozushima were clearly shown by several studies: 2–13 km determined by Ocean Bottom Seismometers (OBS) for the time period between 08/07/2000 and 02/08/2000 (Sakai et al. 2001), 5–20 km by OBS for 11/07/2000 and 31/07/2000 (Nishizawa et al. 2002), 3–20 km by OBS for 21/01/2001 and 13/02/2001 (Nishizawa et al. 2002) and 5–22 km by land networks for 26/06/2001 and 15/07/2001 (Uhira et al. 2005).

Wide-angle seismic refraction surveys, which were conducted four months after the swarm initiation, discovered relatively low P-wave velocity zones in the upper crust between Kozushima and Miyakejima (Kodaira et al. 2002; Nishizawa et al. 2002) and an intra-crustal reflection phase immediately below the swarm (Kodaira et al. 2002).

The seismic reflection data in the present study were obtained by *KR00-08 Cruise of RV Kairei* of Japan Agency for Marine-Earth Science and Technology (JAMSTEC) from 21 to 27 November in 2000, five months after the swarm initiation (Tsuru and Fujie 2006). A total of 250-km-long seismic reflection data were collected in the study area (Fig. 1). The data acquisition was conducted using eight 25-L air-guns with shot spacing of 50 m and a 156-channel streamer cable with group interval of 25 m (Appendix Table 1). The maximum offset length was 4.1 km. Although the maximum offset length seems to be too short to analyze velocity in depths greater than 4 km, large offset length is not necessarily required to



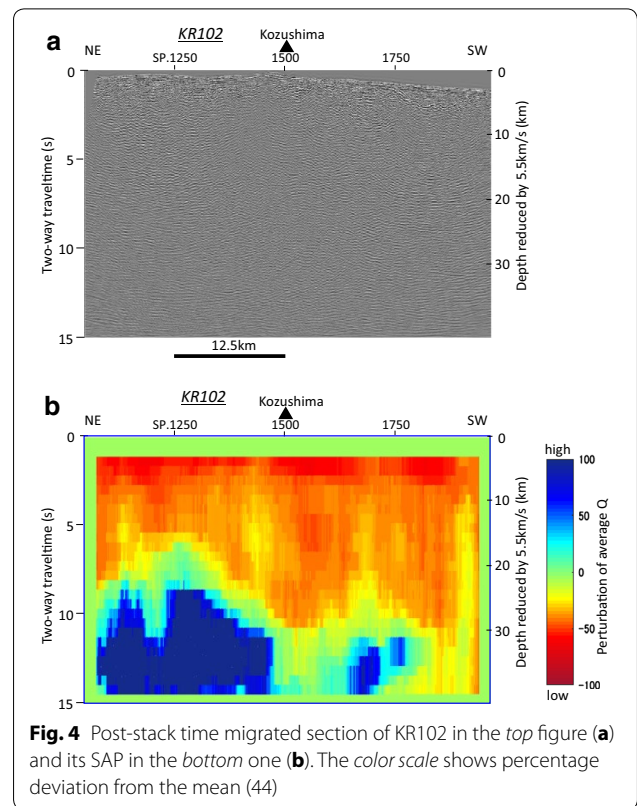
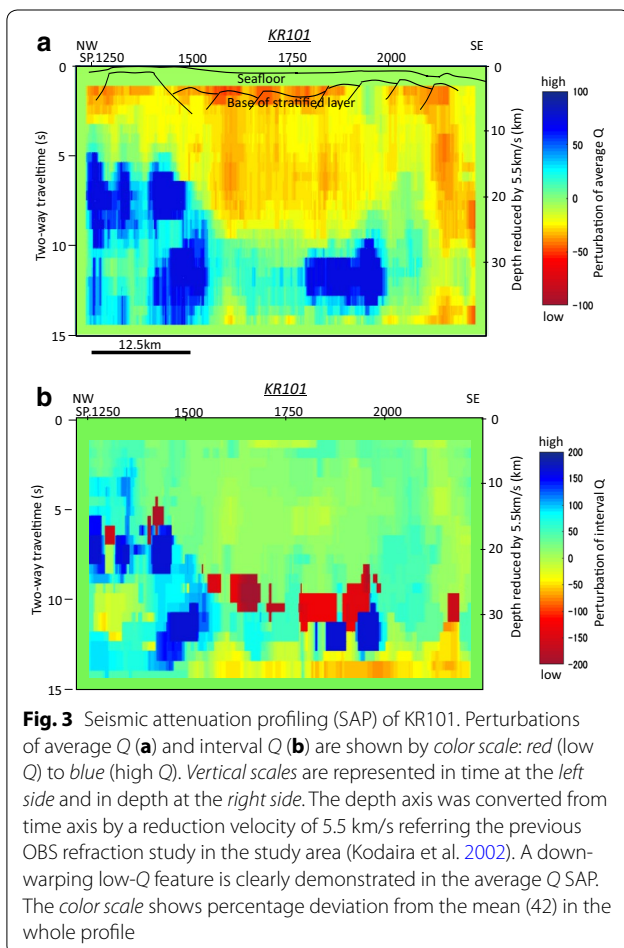
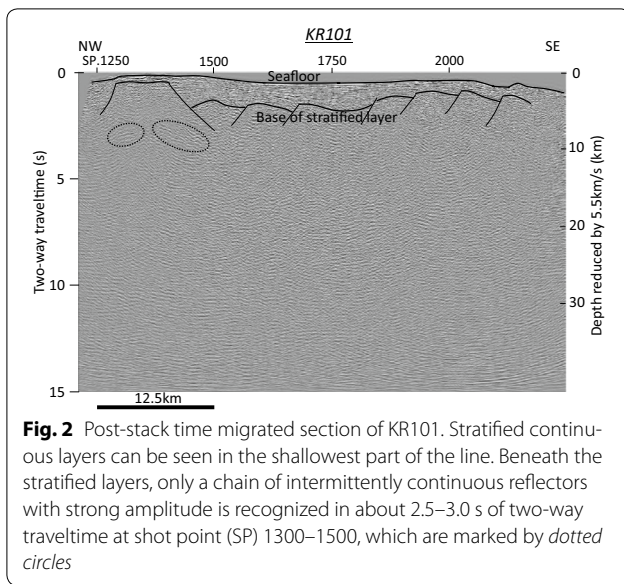
estimate attenuation property by spectral ratio method because frequency distortions caused by NMO corrections become large as offset length increases.

The streamer cable was towed 20 m below the sea surface to avoid the effect of sea-wave noise by seasonal wind that was blowing during the whole survey period. Figure 2 shows a post-stack time migrated profile of the line KR101, which was produced by careful trace editing, deconvolution, NMO correction, multiple suppression, CDP stacking, post-stack time migration and so on (Appendix Fig. 11). As a result, stratified continuous reflections can be observed in the shallowest part of the line. Almost energy of multiples appears to be suppressed. These processing results indicate that the processing was successful. However, almost all parts of the reflection profile below the shallowest stratified reflectors are less reflective, except a chain of intermittently continuous reflectors with strong amplitude in about 2.5–3.0 s of two-way traveltime at shot point (SP) 1300–1500 on the line KR101.

### Results of SAP application

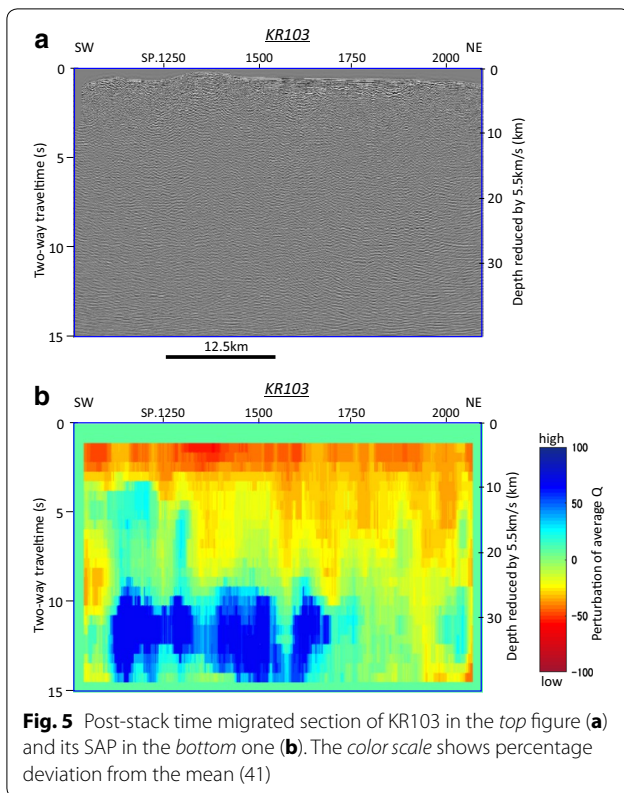
As input data of SAP calculation, post-stack migrated records were used in the present study. Post-stack data have an advantage from the viewpoint of  $S/N$  ratio because random noise and remaining multiples are strongly suppressed by stacking effect, and reversely it has a disadvantage in preservation of original frequency contents because NMO correction distorts frequency of reflection even if the NMO velocity is correct. On the other hand, pre-stack data have a disadvantage in  $S/N$  ratio, and reversely it has an advantage in frequency preservation.  $S/N$  ratio of the seismic reflection data from KR00-08 Cruise is not so high due to the seasonal wind as mentioned in “Study area and data specifications” section, and therefore, the post-stack data were selected as the input data for SAP computation in the present study. Also, frequency distortion caused by NMO correction is not so large in the depths below 10 km (Appendix 2).

SAP profiles were computed for all the seismic lines. As shown in Figs. 3, 4, 5 and 6, a common attenuation feature



can be seen in all of the SAP profiles: The shallower parts show relatively high attenuation, while the deeper parts relatively low attenuation. However, this common feature does not fit with attenuation feature in the depths below approximately 35 km, which may be a limitation of SAP application to the present dataset. Among them, the SAP profile of average Q on the line KR101 indicates the most remarkable feature: a down-warping high-attenuation zone shown by red-to-yellow colors (Fig. 3a). Comparing Figs. 2 and 3a, it is clearly understood that a remarkable spatial variation in attenuation property showed up on the poorly reflective area below the shallowest stratified layers.

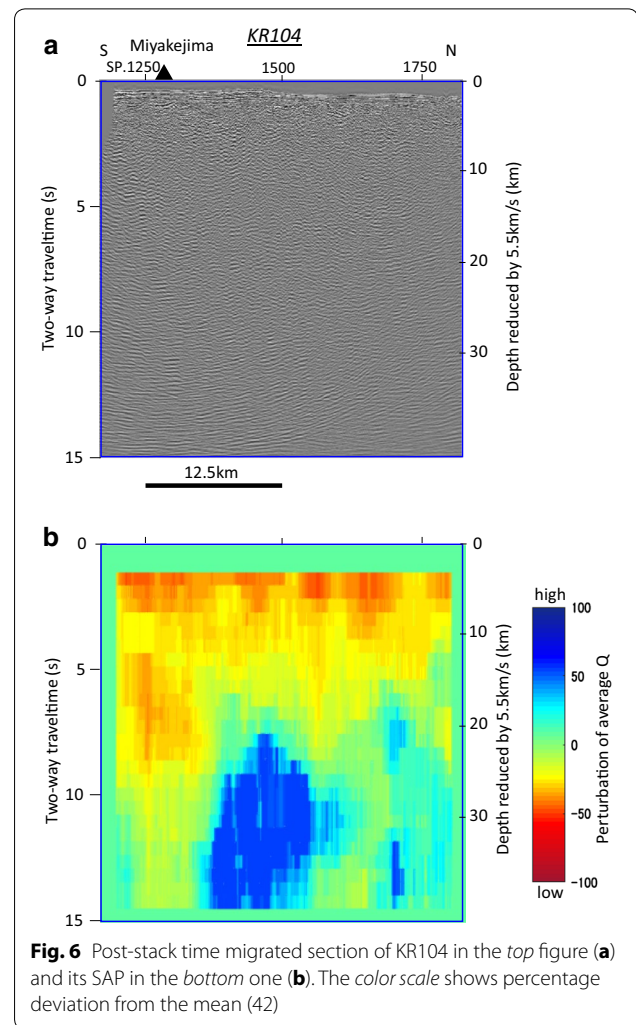
Figure 3b shows SAP profile of interval Q, which came out of the average Q values of Fig. 3a. Abnormally large interval Q values can be recognized locally along the lower boundary of the down-warping high-attenuation zone detected on the average Q SAP profile. Drastic change in the average Q near the lower boundary of the high-attenuation zone caused the abnormally large interval Q values. This result indicates difficulty in the conversion from average Q to interval Q by SAP for the seismic reflection data used in the present study, and we therefore use average Q SAP profiles in the following discussions.



Figures 4, 5 and 6 show both the reflection profiles and average  $Q$  SAP profiles of KR102–KR104, and every SAP profile does not show such a remarkable variation in attenuation as that of KR101 has demonstrated. However, although it is a little vague, down-warping high-attenuation features seem to be imaged on both KR102 and KR103. Regarding KR104 and KR101, relatively high-attenuation areas can be seen in the southern half of the line and in the southeast end of the line, respectively, which are segments that pass near the volcanic edifice of the Miyakejima.

### Discussion

Here we discuss whether or not SAP method is applicable to tectonic study in volcanic area and whether or not the down-warping high-attenuation feature reflects any subsurface structures. In the present study, we assumed that spatial variation in reflectivity is so small over the poorly reflective area that the spatial variation in reflectivity does not affect that in attenuation. In a drastic way



of expression, the reflectivity can be assumed almost uniform within the poorly reflective area, for wavelength used in the seismic reflection survey. It is therefore considered that the observed down-warping high-attenuation feature has no relationship with variation in reflectivity.

As shown in Figs. 3, 4, 5 and 6, every SAP profile shows a trend that the uppermost part has the highest attenuation. Although the top of each SAP profile was placed by zeros due to the unsuitable condition of spectral ratio computation in water layer, the areas of the highest attenuation can be correlated with the lower half of the stratified layers on the reflection profiles.

The areas can be interpreted as volcanoclastic layers from the sedimentological point of view around the study area. Moreover, every SAP profile has a common attenuation feature that the shallower parts show relatively high attenuation while the deeper parts relatively low attenuation, which is consistent to a general attenuation structure in the crust. The above-mentioned characteristics commonly observed on every SAP profile can be considered to be one of the evidences that this method is applicable to tectonic study in poorly reflective area, in addition to previous studies in the oil industry (e.g., Tsuru et al. 2014; Zhou et al. 2011), if the down-warping high-attenuation feature were reasonably explained.

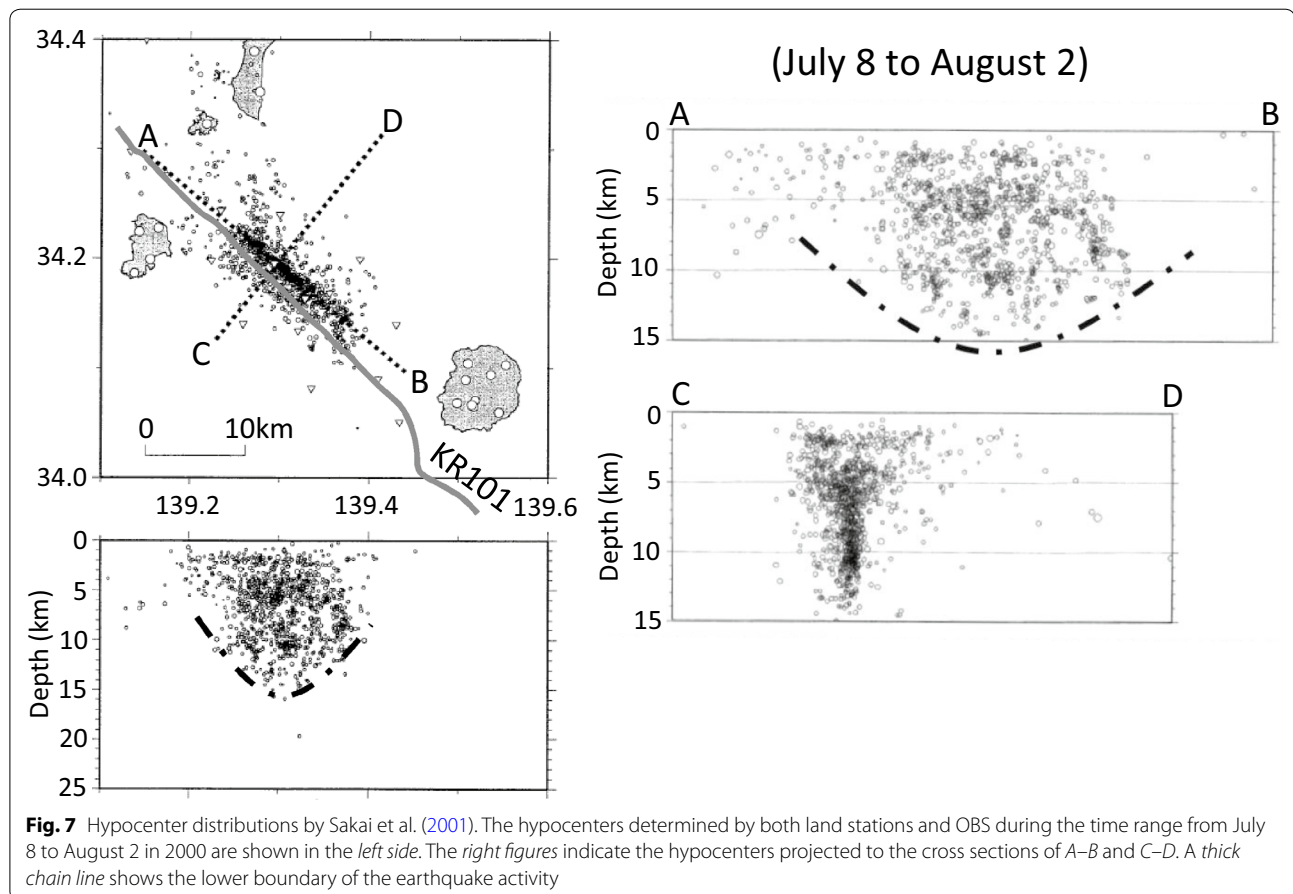
Regarding the down-warping feature of high-attenuation zone along the line KR101, the following two tectonic factors would be considered as candidates of the possible causes:

1. sedimentary rocks such as volcanoclastic rocks that deposited between two volcanos: Miyakejima and Kozushima,

2. relatively porous and/or fractured zones within volcanic basement.

As for the former, no reflections can be seen on the relevant part of the reflection profile (Fig. 2). Moreover, no volcanoclastic layers that reach 20 km in thickness have been observed on any seismic lines in the study area. Therefore, we eliminate the former from discussion and examine possibility of the latter below.

As mentioned above, the largest earthquake swarm ever recorded in Japan occurred between Miyakejima and Kozushima during the two months from June 26, 2000. The swarm initiated beneath the southwest flank of Miyakejima and then migrated northwestward toward the direction of Kozushima. Sakai et al. (2001) reported the hypocenter distribution determined by both land stations and Ocean Bottom Seismometers (OBS) during the period of time from July 8 to August 2, 2000 (Fig. 7). Nishizawa et al. (2002) showed the hypocenters determined by OBS from July 11 to 31 in 2000 and from January 21 to February 13 in 2001 (Fig. 8). Uhira et al. (2005) reported the hypocenters relocated by a station



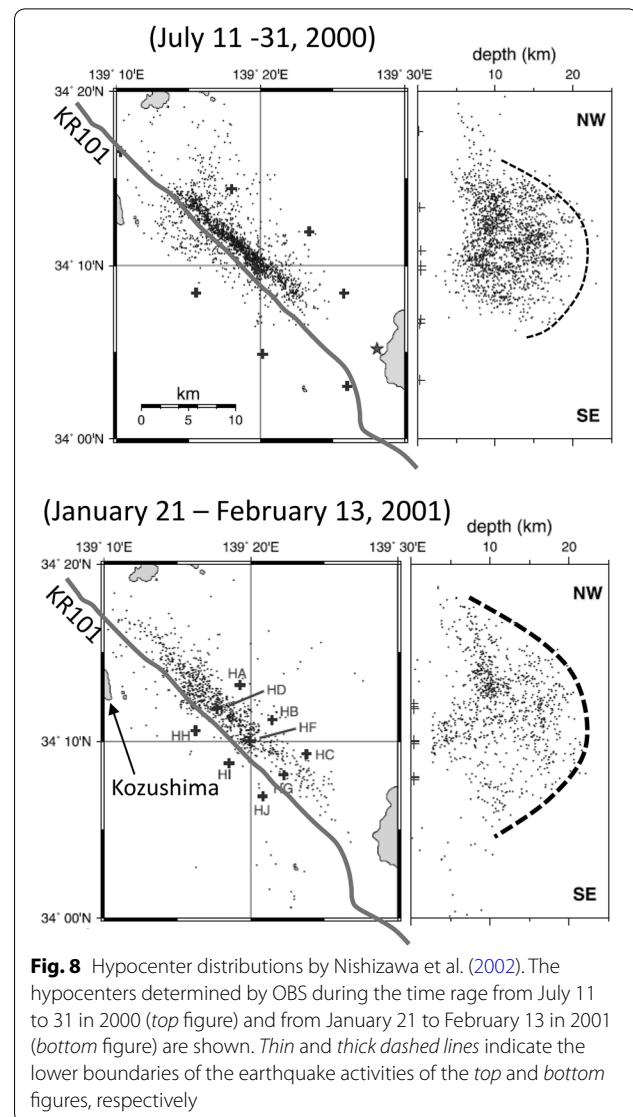
correction method and a double-difference method for earthquakes determined by land stations from June 26 to July 15 in 2000 (Fig. 9). Strike-slip focal mechanism with NW–SE compression axis is predominant for the swarm earthquakes (Sakai et al. 2001; Uhira et al. 2005).

Here we compared the hypocenter distributions with the down-warping high-attenuation zone on SAP profile of KR101 in Fig. 10. The lower boundaries of the above-mentioned four kinds of hypocenter distributions are indicated as a thick chain line, a thin dashed line, a thick dashed line and a dotted line, respectively.

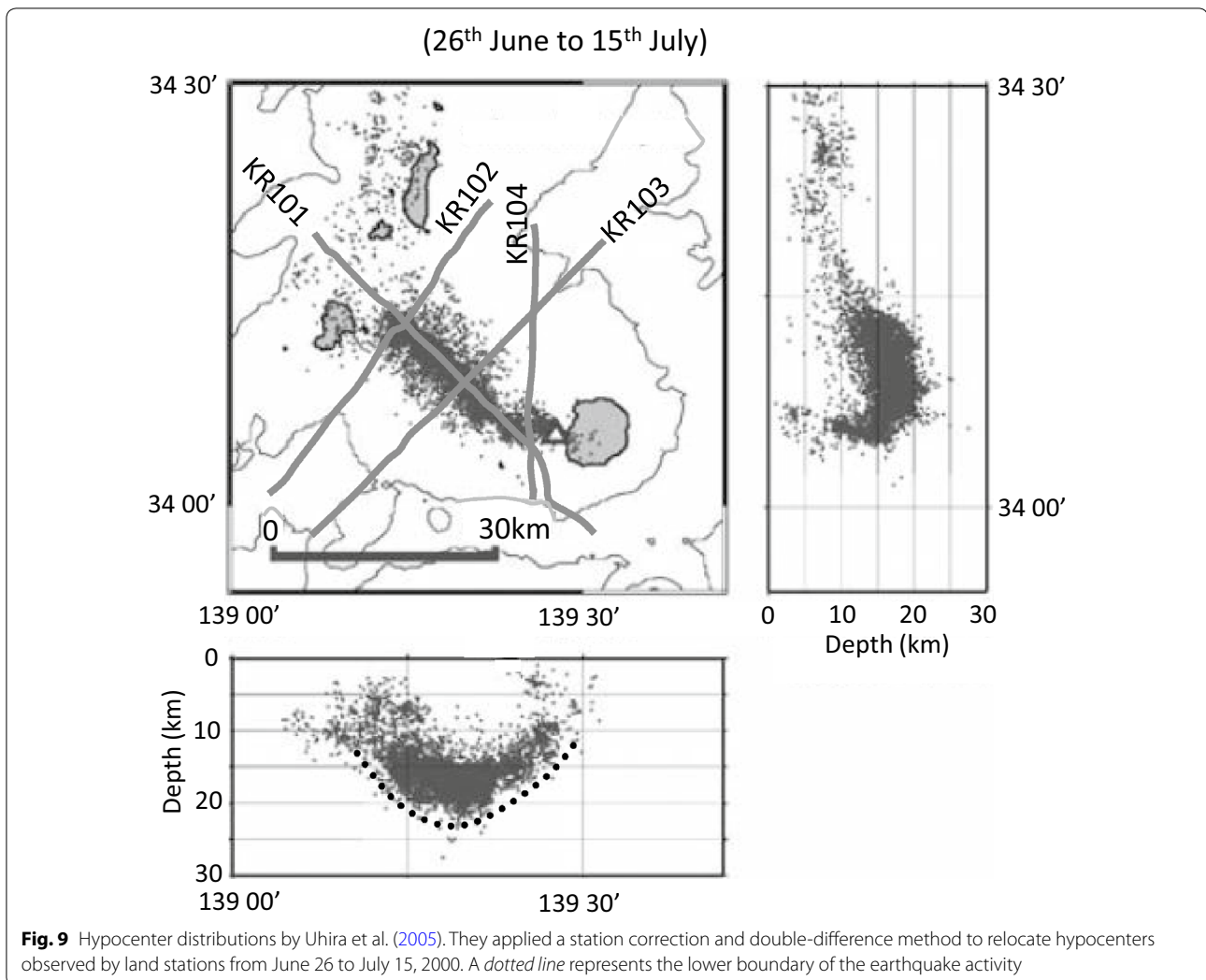
As shown in Fig. 10, every hypocenter distribution indicates a down-warping feature on the NW–SE section, which is similar in shape with that of high-attenuation zone on the SAP profile of KR101. Particularly, those features resulted from OBS networks deployed above the earthquake swarm (Sakai et al. 2001; Nishizawa et al. 2002) are important in evaluating the shape and depth of hypocenter distribution. On the other hand, the hypocenter distribution of Uhira et al. (2005) may be strictly inappropriate to evaluate the shape and depth of the swarm activity because it was determined by land network. However, its distribution is indispensable to investigate the early stage of the 2000 swarm activity that initiated from the Miyakejima side.

Thus, the down-warping high-attenuation zone on the SAP profile is appeared to reflect the 2000 swarm area, which would be dominated by fractures, from the similarity in shape. However, considering the difference in depth between the high-attenuation zone and the hypocenter distributions from OBS networks, it would be impossible that the high-attenuation zone is explained by only the 2000 swarm. Accordingly, we concluded that the down-warping high-attenuation zone observed on the SAP profile of KR101 reflects a fractured area that were developed by magma activity responsible for the earthquake swarms that have been repeatedly occurring between Miyakejima and Kozushima.

This conclusion can be supported by the low-velocity zones that were specified by the wide-angle seismic refraction surveys (Kodaira et al. 2002; Nishizawa et al. 2002), because seismic attenuation is correlated with seismic velocity (Tompkins and Christensen 2001; Tsuji and Iturrino 2008). However, why is not the dominant down-warping high-attenuation feature observed on the lines KR102–104? Although this issue is difficult to be



revealed due to the limited data, we interpret that this may be caused by the difference in distance of ray paths that have influence on attenuation. As shown in Fig. 7, the deeper events (>7 km) of the swarm form a very thin (2 km thick) plane of a NW–SE strike and a vertical dip (Sakai et al. 2001), like a flower structure consisting of strike-slip faults. The seismic reflection waves collected on the lines KR102–104 should get across the plane, while those on the KR101 should propagate through the plane.



Accordingly, the most predominant high-attenuation feature would be shown up on a seismic line running over and along the thin plane.

### Conclusions

The present study suggested a possibility that the seismic attenuation profiling (SAP) can map physical properties

of rocks in poorly reflective area such as volcanic area, where seismic reflection profile is difficult to provide structural information or physical properties because of very few reflections.

The down-warping high-attenuation zone was mapped by SAP between Miyakejima and Kozushima. This would reflect a fractured area that was developed

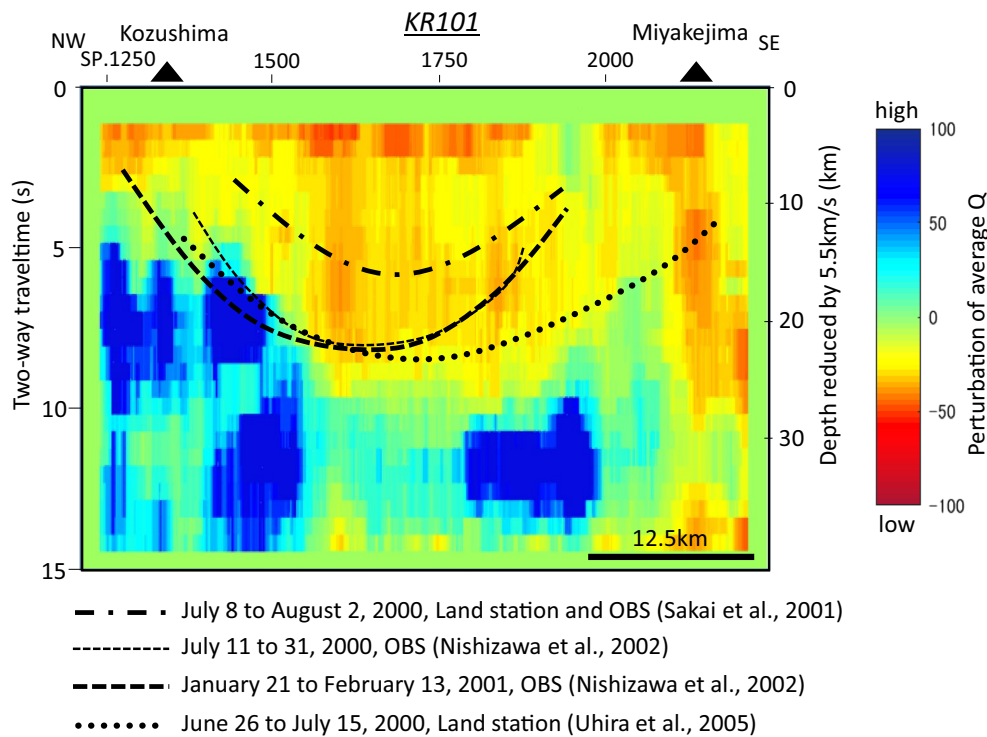


**Fig. 10** Hypocenter distributions by previous studies were compared with the down-warping high-attenuation zone specified on SAP of KR101. The color scale shows percentage deviation from the mean. The lower boundaries of the hypocenter distributions of Sakai et al. (2001), the 1st observation of Nishizawa et al. (2002), 2nd observation of Nishizawa et al. (2002) and Uhira et al. (2005) are indicated as a thick chain line, a thin dashed line, a thick dashed line and a dotted line, respectively

by magma activity responsible for the earthquake swarms that have been repeatedly occurring there. The zone is also consistent with the low-velocity zone deduced from the previous wide-angle seismic refraction studies.

#### Authors' contributions

TT is responsible in the whole part of the manuscript. TN conducted a part of the data processing of the seismic reflection data and contributed to the interpretation and the discussions. GF contributed to the data acquisition of the seismic reflection data, a part of the SAP calculation procedure and the discussions. All authors read and approved the final manuscript.

#### Author details

<sup>1</sup> Academic Assembly, Tokyo University of Marine Science and Technology (TUMSAT), 5-7, Konan 4-chome, Minato-ku, Tokyo 108-8477, Japan. <sup>2</sup> Research and Development Center for Earthquake and Tsunami, Japan Agency for Marine-Earth Science and Technology (JAMSTEC), 3173-25 Showa-machi, Kanazawa-ku, Yokohama 236-0001, Japan.

#### Acknowledgements

Thanks are due to JAMSTEC for disclosure of the seismic reflection data of *KR00-08 survey* and Captains, Seismic Party, and the crew of the *R/V KAIREI* for their efforts to acquire data of good quality in difficult weather conditions. We are deeply grateful for Editor Dr. Yosuke Aoki and two anonymous

referees whose comments and suggestions helped to improve and clarify the manuscript. The survey was conducted as JAMSTEC Frontier Research Program for Subduction Dynamics and a research program supported Special Coordination Funds of the Ministry of Education, Culture, Sports, Science and Technology of Japan.

#### Competing interests

The authors declare that they have no competing interests.

#### Appendix 1

The purpose of this "Appendix" is to provide additional explanations of the seismic reflection survey in 2000 as well as to show a typical amplitude spectrum used in the present study. The seismic line specifications and the data acquisition parameters are summarized in Table 1. The data processing flow and the processing parameters for each sequence are represented in Fig. 11. An amplitude spectrum is shown in Fig. 12, as a reference of the denominator of the left side of Eq. (5). The spectrum was computed by summing amplitude spectrums, which were extracted in 2.5–3.0 s of two-way traveltime at SPs 1720–1740 on line KR101.

**Table 1 Seismic line specifications and data acquisition parameters**

Line name	Line length	Direction	Shot point
KR101	50.0 km	NW → SE	1250–2250
KR102	44.7 km	NE → SW	1082–1976
KR103	52.25 km	SW → NE	1045–2090
KR104	30.65 km	S → N	1207–1820
Observation period	November 21–27, 2000		
Vessel	<i>R/V Kairei</i>		
Source	Air-gun array, 8 × 1500 cu. in., 2000 psi, towing depth 10 m		
Shot spacing	50 m		
Receiver	Streamer cable, 156 channel, array hydrophones (32 phones/channel), towing depth 20 m		
Receiver spacing	25 m		
Source–receiver offset length	200–4100 m		
Sampling rate	4 ms		
Record length	15 s		

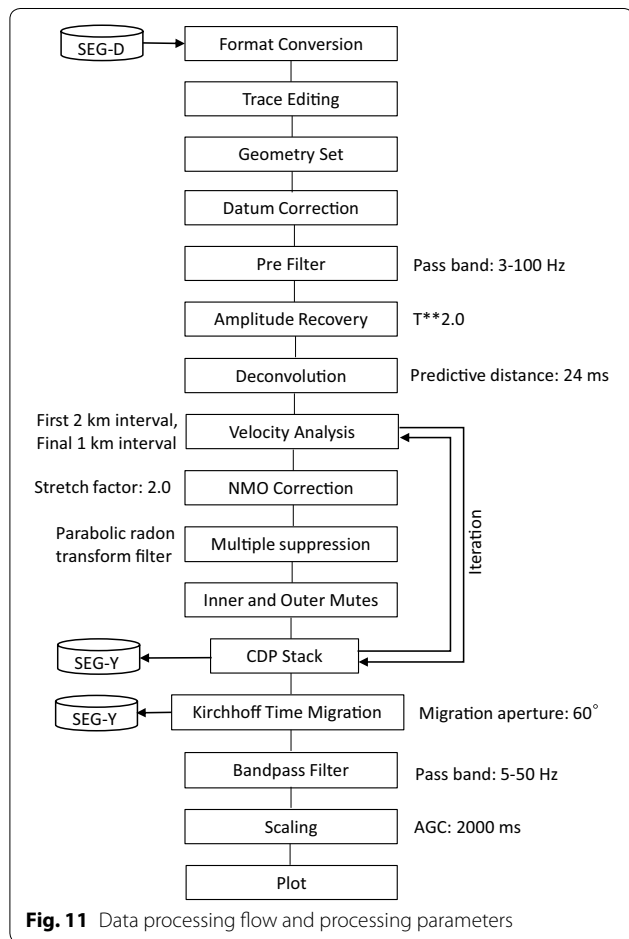


**Fig. 11** Data processing flow and processing parameters

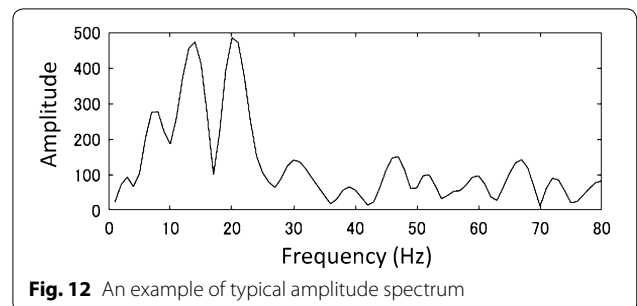


**Fig. 12** An example of typical amplitude spectrum

**Appendix 2**

Spectrum distortion by NMO correction is examined in this “Appendix.” Errors in average *Q* values for several source–receiver offsets due to frequency distortion are examined by using pre- and post-NMO traces under the data acquisition geometry of the present study, assuming a constant velocity of 5 km/s. As shown in Table 2, the errors are less than 9% in 10 km depth, 5.5% in 15 km depth and 4% in 20 km depth. Since the errors on pre-NMO traces are averaged by CDP stacking, those of post-NMO (stacked) traces would be estimated 5% or less in case of the present study.

Received: 22 August 2016 Accepted: 20 December 2016

Published online: 03 January 2017

**Table 2 Average Q values calculated by spectral ratio using pre- and post-NMO traces**

Depth	Pre-NMO	Post-NMO offset = 1 km	Post-NMO offset = 2 km	Post-NMO offset = 3 km	Post-NMO offset = 4 km
10 km	100.0	100.5	101.9	104.5	109.0
15 km	100.0	100.3	101.2	102.9	105.5
20 km	100.0	100.2	100.9	102.1	104.0

## References

- Dasgupta R, Clark RA (1998) Estimation of Q from surface seismic reflection data. *Geophysics* 63:2120–2128
- Hamada N (2001) A history of seismic activity around Miyakejima, Kozushima and Niiijima, the northern Izu islands. *J Geogr* 110:132–144 **(in Japanese with English abstract)**
- Hamada N, Tanaka Y, Nishide N (1985) Detailed comparison of seismic activities associated with the 1962 and the 1983 eruption of Miyake-jima. *Bull Volcanol Soc Jpn* 30:147–160
- Hauge PS (1981) Measurements of attenuation from vertical seismic profiles. *Geophysics* 46:1548–1558
- Japan Meteorological Agency (2000) Recent seismic activity in the Miyakejima and Niiijima–Kozushima region, Japan: the largest earthquake swarm ever recorded. *Earth Planets Space*, 53(8):i–viii. doi:10.1186/BF03351657
- Knopoff L (1964) Q. *Rev Geophys* 2:625–660. doi:10.1029/RG002i004p00625
- Kodaira S, Uehira K, Tsuru T, Sugioka Y, Suyehiro K, Kaneda Y (2002) Seismic image and its implications for an earthquake swarm at an active volcanic region off the Miyake-jima–Kozu-shima, Japan. *Geophys Res Lett* 29:43.1–43.4
- Matsushima J (2006) Seismic wave attenuation in methane hydrate-bearing sediments: vertical seismic profiling data from the Nankai Trough exploratory well, offshore Tokai, central Japan. *Geophys Res Lett* 33:L03306. doi:10.1029/2005GL024466. [Correction, *Geophys Res Lett* 33:L02305. doi:10.1029/2005GL024466, 2006]
- Mavko GM, Nur A (1979) Wave attenuation in partially saturated rocks. *Geophysics* 44:161–178
- Mikada H, Watanabe H, Sakashita S (1997) Evidence for subsurface magma bodies beneath Izu-Oshima, volcano inferred from a seismic scattering analysis and possible interpretation of the magma plumbing system of the 1986 eruptive activity. *Phys Earth Planet Inter* 104:257–269
- Mogi K (1963) Some discussion of after shocks, fore shocks and earthquake swarms. *Bull Earthq Res Inst Univ Tokyo* 41:615–618
- Nishizawa A, Ono T, Otani Y (2002) Seismicity and crustal structure related to the Miyake-jima volcanic activity in 2000. *Geophys Res Lett* 29:12.1–12.4
- Sakai S, Yamada T, Ide S, Mochizuki M, Shiobara H, Urabe T, Hirata N, Shinohara M, Kanazawa T, Nishizawa A, Fujie G, Mikada H (2001) Magma migration from the point of view of seismic activity in the volcanism of Miyake-jima island in 2000. *J Geophys* 110:145–155 **(in Japanese with English abstract)**
- Spencer TW, Sonnad JR, Butler TM (1982) Seismic Q-stratigraphy or dissipation. *Geophysics* 47:16–24
- Tokuyama H, Suyehiro K, Watanabe H, Ohnishi M, Takahashi A, Ikawa T, Asada M, Fujioka K, Ashi J, Kuramoto S, Soh W, Ogawa Y (1988) Multichannel seismic reflection profile from south of the Izu Oshima. *Kazan* 33:67–77 **(in Japanese with English abstract)**
- Tompkins MJ, Christensen NI (2001) Ultrasonic P- and S-wave attenuation in oceanic basalt. *Geophys J Int* 145:172–186
- Tonn R (1991) The determination of seismic quality factor Q from VSP data: a comparison of different computational methods. *Geophys. Prosp.* 39:1–27
- Tsuji T, Iturrino GJ (2008) Velocity-porosity relationships in oceanic basalt from eastern flank of the Juan de Fuca Ridge: the effect of crack closure on seismic velocity. *Explor Geophys* 39:41–51
- Tsukui M, Suzuki Y (1998) Eruptive history of Miyakejima volcano during the last 7000 years. *Bull Volcanol Soc Jpn* 43:149–166 **(in Japanese with English abstract)**
- Tsuru T, Fujie G (2006) Reflective body observed by multi-channel reflection survey off Niiijima and Kozushima, Japan. *JAMSTEC R&D* 3:53–60
- Tsuru T, No T (2011) Seismic attenuation attribute and its implication to physical property analyses in less-reflective areas. In: Proceedings of the 10th SEGJ international symposium, pp 151–154
- Tsuru T, Sasaki A, Urabe S (2014) Fault seal evaluation by using attenuation effects of seismic reflection data. *J Jpn Assoc Petrol Technol* 79:54–62 **(in Japanese with English abstract)**
- Uehira K, Baba T, Mori M, Katayama H, Hamada N (2005) Earthquake swarms preceding the 2000 eruption of Miyakejima volcano. *Jpn Bull Volcanol* 67:219–230
- Worthington MH, Hudson JA (2000) Fault properties from seismic Q. *Geophys J Int* 143:937–944
- Zhou J, Birdus S, Hung B, Teng KH, Xie Y, Chagalov D, Cheang A, Wellen D, Garrity J (2011). Compensating attenuation due to shallow gas through Q tomography and Q-PSDM, a case study in Brazil. Expanded abstract, 2011 SEG annual meeting

Submit your manuscript to a SpringerOpen® journal and benefit from:

- Convenient online submission
- Rigorous peer review
- Immediate publication on acceptance
- Open access: articles freely available online
- High visibility within the field
- Retaining the copyright to your article

Submit your next manuscript at ► [springeropen.com](http://springeropen.com)